

See discussions, stats, and author profiles for this publication at: <https://www.researchgate.net/publication/358582226>

Quantum image representation: a review

Preprint · February 2022

CITATIONS

0

READS

520

2 authors:



[Marina Lisnichenko](#)

Innopolis University

13 PUBLICATIONS 1 CITATION

[SEE PROFILE](#)



[Stanislav Protasov](#)

Innopolis University

36 PUBLICATIONS 197 CITATIONS

[SEE PROFILE](#)

Some of the authors of this publication are also working on these related projects:





Medical imaging [View project](#)



Thesaurus [View project](#)

Quantum Image Representation: A Review

Marina Lisnichenko MSc ^{1*} and Dr Stanislav Protasov PhD
¹

MLKR Laboratory, Innopolis University, Universitetskaya,
Innopolis, 420500, Tatarstan Republic, Russia.

*Corresponding author(s). E-mail(s):

m.lisnichenko@innopolis.university;

Contributing authors: s.protasov@innopolis.ru;

Abstract

Quantum programs allow to process multiple bits of information at the same time, which is useful in multidimensional data handling. Images are an example of such multidimensional data. Our work reviews 14 quantum image encoding works and compares implementations of 8 of them by 3 metrics: number of utilized qubits, quantum circuit depth, and quantum volume. Our work includes a practical comparison of $2^n \times 2^n$ images encoding, where n varies from 1 up to 8. We observed that Qubit Lattice approach shows the minimum circuit depth as well as quantum volume, Flexible Representation of Quantum Images (FRQI) utilizes the minimum number of qubits. If to talk about variety of processing techniques, FRQI and Novel Enhanced Quantum Representation (NEQR) representations are the most fruitful. As far as quantum computers are limited in qubit number, we concluded that almost all approaches except Qubit Lattice are promising for the near future of quantum image representation and processing. From the point of view of the quantum depth, discrete methods showed the most appropriate result.

Keywords: quantum images, complexity, quantum algorithms, quantum image processing

1 Introduction

Quantum computation is a rapidly developing field. In 2021 private capital investments in quantum computations exceeded \$3B [1]. Due to the quantum parallelism the information processing is performed potentially faster. Acceleration of the calculations through parallelism is highly relevant to multidimensional data, including images. In the quantum programs, images are usually represented in the same way as in classical machines – with pixel coordinates and pixel intensities, but amplitude and phase encodings use different physical parameters for these values. In this work, we compare 14 ways of image encoding including methods: with quantum state amplitudes – amplitude-angular (continuous), qubit binary – amplitude-state (discrete), mixed, and phase image representations. We implemented 8 core representation techniques (other methods are derived or equivalent to the implemented and share their characteristics) for the practical comparison¹. Our survey covers the following quantum image representation methods:

- qubit lattice [2] (2003);
- real ket [3] (2005);
- flexible representation of quantum images - FRQI [4] (2011);
- multi-channel representation for images - MCRQI [5] (2011);
- novel enhanced quantum representation of digital images - NEQR [6] (2013);
- quantum states for M colors and quantum states for N coordinates - QSMC and QSNQ [7] (2013);
- a simple quantum representation - SQR [8] (2014);
- normal arbitrary quantum superposition state - NAQSS [9] (2014);
- generalized quantum image representation - GQIR [10] (2015);
- quantum representation of multi wavelength images - QRMW [11] (2018);
- quantum image representation based on bitplanes - BRQI [12] (2018);
- order-encoded quantum image model - OQIM [13] (2019);
- quantum representation of indexed images and its applications - QIIR [14] (2020);
- Fourier transform qubit representation - FTQR [15] (2020).

The review contains the information about quantum image representation methods and applicable image processing techniques. To compare the methods, we use 3 parameters:

- *number of utilized qubits* - each existing computer is limited in number of qubits and this number defines the possibility of algorithm execution;
- *circuit depth* - length of the longest quantum gate path from the zero-state to the end of the encoding procedure. The bigger the depth is, the more errors affect on the output result quality. This metric is an analogy of the classical time complexity;
- *quantum volume* - squared minimum between the circuit depth and number of qubits. This metric varies for different quantum machines, and

¹github.com/UralmashFox/QPI

depends on the base gates. Quantum volume is an integral metric which allows to evaluate a computing capability with a single quantity.

In conclusion 3 we sum the observed information and make a statement about future work.

2 Quantum image representation (QIR) techniques

We identified four major ways of quantum image representation: **continuous amplitude** representation, where pixel intensity is encoded with quantum state amplitude p , corresponding to observation probability p^2 , **amplitude with binary intensity** representation (discrete), **mixed**, and **phase intensity** representation. Figure 1 shows the suggested classification.

Continuous representation allows to use a single qubit for intensity or coordinate encoding. This is the main advantage of the methods. Multiple measurements are required to estimate the pixel intensity with high precision.

In the discrete intensity representation, oppositely, each state corresponds to separate intensity or coordinate bit-value. Measurement result contains accurate data expansion of a single pixel data.

Mixed representations either store pixel coordinates discretely or do not encode coordinate.

Phase encoding uses continuous representation, but in an XY Bloch sphere projection plane.

In the following subsections, we describe each approach separately.

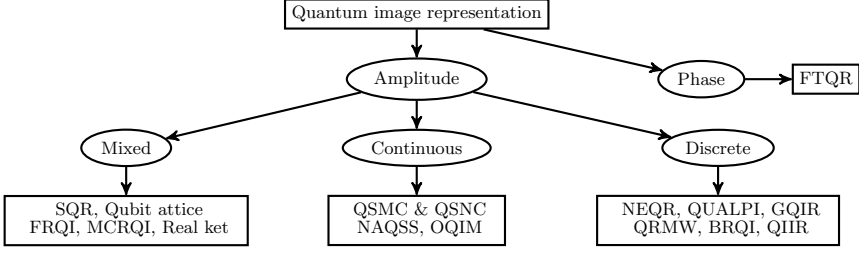
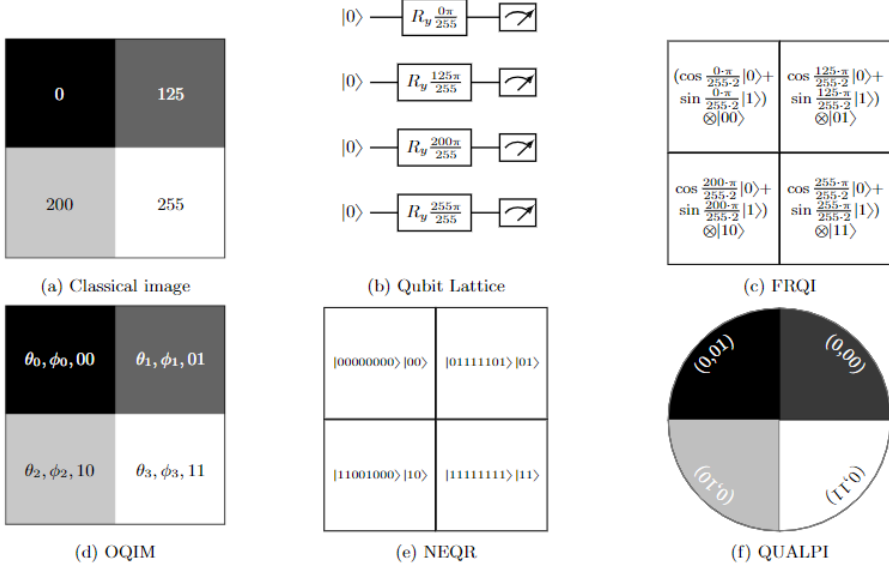
2.1 Mixed representation

The chapter describes quantum image representation algorithms based on both discrete and continuous methods. It's common for mixed methods where continuous encoding is used for the pixel intensity and the pixel location is represented discretely. We also include Qubit Lattice and SQR algorithms, however these methods do not have a specific coordinate encoding procedure.

2.1.1 Qubit Lattice

Venegas-Andraca and Bose [2] did a major preparatory work in the quantum image representation and processing. The paper describes the basic quantum definitions and measured results interpretation. Proposed image representation is naïve and consists of literally copying the classical representation into quantum. Authors suggest to use R_y rotation gate to set each pixel's intensity. Therefore, the number of utilized qubits is 2^{2n} where $2^n \times 2^n$ is an image size. Figure 2b shows an example of encoding the image with pixel intensities $\{0, 125, 200, 255\}$.

Coordinate qubits absence and quantum circuit simplicity are the strong sides of the encoding method. Due to simplicity, authors of quantum convolutional neural networks papers actively utilize this representation method (or

**Fig. 1:** Quantum image representation (QIR) classification**Fig. 2:** (a) Classical image and (b-f) quantum image representations

modified) even if it is not evidently claimed [16], [17], [18]. At the same time, classical image processing based on Qubit Lattice did not spread. The approach has strong negative sides such as big number of used qubits and small number of known processing methods. However, for the sake of justice, it is the first formulation of quantum image storing.

2.1.2 FRQI

Authors [4] use the continuous amplitude encoding with intensity-to-amplitude representation.

$$|I(\alpha)\rangle = \frac{1}{2^n} \sum_{i=0}^{2^{2n}-1} (\cos\alpha_i |0\rangle + \sin\alpha_i |1\rangle) \otimes |i\rangle \quad (1)$$

where $|I(\alpha)\rangle$ is a quantum image representation, α is a parameter responsible for intensity and equal to a half of R_y rotation angle, $|i\rangle$ represents the pixel coordinate binary expansion. The greater α is, the closer pixel intensity to the

maximum. Therefore, the precision of the intensity estimation depends on the number of circuit executions.

Figure 2c shows the image with pixel intensities $\{0, 125, 200, 255\}$. The image representation code is available in our repository.

The FRQI implies a huge number of processing algorithms. For example, the paper presents processing algorithms that affect intensity, coordinate, or both intensity and coordinate. The first processing group changes all the pixel intensities, the second group changes intensity at some locations, the last group "targets information about both color and position as in Fourier transform". Moreover, multi-channel expansion [19], image compression, line detection [4], binarization, histogram computing, histogram equalization [20], global and local translation designs [21] are also available for FRQI. The image representation technique maintains comprehensive processing such as information hiding [22], Richardson-Lucy image restoration [23], multilevel segmentation [24], hybrid images creating [25]. Additionally, FRQI helps to find correlation property of multipartite quantum image [26], implement image fusion [27], encrypt images via algorithm based on Arnold scrambling and wavelet transforms [28].

At the same time, FRQI has the following drawbacks:

- due to the single intensity qubit "some digital image-processing operations for example certain complex color operations", are impossible (such as "partial color operations and statistical color operations") [6].
- circuit depth is $O(2^{4n})$ for $2^n \times 2^n$ image [6].

FRQI is beneficial for the applications with limited qubit number and does not demand high intensity precision. FRQI supports broad spectrum of quantum image processing techniques useful for basic image processing. However the continuous intensity representation approach may limit such processing algorithms as edge detection and texture features.

2.1.3 MCRQI

The authors of [5] apply FRQI 2.1.2 approach to the $RGB\alpha$ images, where α is a transparency channel. The difference is in the number of qubits used to encode an intensity. Authors represent the multichannel image as follows:

$$|I(\theta)\rangle = \frac{1}{2^n} \sum_{i=0}^{2^{2n}-1} |c_{RGB\alpha}^i\rangle \otimes |i\rangle \quad (2)$$

where $|c_{RGB\alpha}^i\rangle$ is a color state and equals to:

$$|c_{RGB\alpha}^i\rangle = \frac{1}{2} \left(\begin{bmatrix} \cos \theta_{Ri} & |0\rangle \\ \sin \theta_{Ri} & |1\rangle \end{bmatrix} \otimes |00\rangle + \begin{bmatrix} \cos \theta_{Gi} & |0\rangle \\ \sin \theta_{Gi} & |1\rangle \end{bmatrix} \otimes |01\rangle + \begin{bmatrix} \cos \theta_{Bi} & |0\rangle \\ \sin \theta_{Bi} & |1\rangle \end{bmatrix} \otimes |10\rangle + \begin{bmatrix} \cos \theta_{\alpha i} & |0\rangle \\ \sin \theta_{\alpha i} & |1\rangle \end{bmatrix} \otimes |11\rangle \right). \quad (3)$$

Multi-channel representation encodes intensities $\in [0, 255]$ with angles $\theta_{Ri}, \theta_{Gi}, \theta_{Bi}, \theta_{\alpha i} \in [0, \frac{\pi}{2}]$ via uniform scaling. As far as image has several channels, authors say about applicability of the one-channel operations for each of them. Authors [29] developed a chromatic framework for quantum movies and provided frame-to-frame and color of interest operations, sub-block swapping. Yan *et al.* described audio-visual synchronisation in quantum movies using MCRQI [30]. Sun *et al.* proposed channel of interest realization, channel-swapping and α blending operations [31]. Hu *et al.* all proposed image encryption based on FRQI modification [28]. The MCRQI has the same pros and cons as the FRQI. Additionally, to get access to each color layer channels r, g, b has to be measured separately.

2.1.4 SQR

The authors [8] combine Qubit Lattice image representation with normalized pixels and NEQR (see 2.3.1) approach of max and minimum pixel values. Instead of pixel intensity authors use "energy" term to show the relation to the infrared images. Their paper describes the Qubit Lattice approach [2] with modifications. Authors of the Qubit Lattice converted intensities directly into angles, while in SQR intensities go through a normalization step first. Suppose, E_{ij} is an energy value detected at the position i, j , E_m minimum energy value, E_M maximum energy value. The normalized energy value is $\tilde{E}_{ij} = \frac{E_{ij} - E_m}{E_M - E_m}$. \tilde{E}_{ij} determines R_y rotation angle via the following expression:

$$\theta_{ij} = 2 \arcsin \tilde{E}_{ij} \quad (4)$$

To encode complete image information, 10 qubits store E_M and E_m energy values. Totally, to encode an image of size $2^n \times 2^n$ algorithm needs $2^n \times 2^n + 10$ qubits.

Authors provide clear explanation of how to convert energy into quantum representation and why is it so intuitive. Due to narrow representation specification, the SQR did not become widespread in terms of processing. Paper describes global and local operations, "retrieval of marked information" (kind of segmentation). However the approach is still "heavy" in qubits.

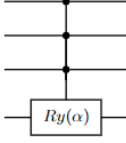
2.1.5 Real Ket

Latorre [3] attempted to separate a pixel's coordinates and intensity into quadrants. The first step of the encoding is to split image into 4 parts (upper-left, upper-right, lower-left, and lower-right). Next, the same step (splitting) repeats until each block contains a quad of pixels. A pair of qubits describes the grid-square pixel coordinate and additional qubit's amplitude holds intensity. This method, as well as FRQI, intensively uses multicontrol R_y gated (Figure 3a), but Real Ket does not have a dedicated intensity qubit. In theorem 8 authors of [32] proved that decomposition of one such k-qubit controlled gate requires 2^k CNOT gates.

Overall, the algorithm requires $2n + 1$ qubits, where $2^n \times 2^n$ is an image size. The final state equation is the following:

$$|\Psi_{2^n \times 2^n}\rangle = \sum_{i_1, \dots, i_n=1, \dots, 4} c_{i_n, \dots, i_1} |i_n, \dots, i_1\rangle. \quad (5)$$

where $|\Psi\rangle$ is a quantum image, c_i pixel intensity, i_n is a representation of the pixel's location corner in the 4×4 grid. Figure 3b gives graphical pixels' coordinates representation for the 4×4 image.



(a) Multicontrol Ry gate

$i_1 = 1$	$i_1 = 2$	$i_1 = 1$	$i_1 = 2$
$i_2 = 1$		$i_2 = 2$	
$i_1 = 3$	$i_1 = 4$	$i_1 = 3$	$i_1 = 4$
$i_2 = 3$		$i_2 = 4$	
$i_1 = 1$	$i_1 = 2$	$i_1 = 1$	$i_1 = 2$
$i_2 = 3$		$i_2 = 4$	
$i_1 = 3$	$i_1 = 4$	$i_1 = 3$	$i_1 = 4$
$i_2 = 3$		$i_2 = 4$	

(b) Real Ket image encoding

Fig. 3: (a) Multicontrol Ry gate (gate consists of 3 control qubits that rotate the last one – target – qubit for an angle α) and (b) Real Ket coordinate estimation.

Authors of the paper describe the image compression algorithm based on Fourier transform. Ma *et al.* proposed quantum Radon transform based on Real Ket encoding [33]. The similar image representation is used for low-rank tensor completion [34].

2.2 Pure continuous representation

Representation algorithms of the current chapter utilize only continuous amplitude encoding for both pixel intensity and coordinates.

2.2.1 QSMC and QSNC

Suppose the image consists of m different pixel intensities taken from M possible (if an image is an 8-bit gray-scaled, $M = 256$), and contains $N = 2^n \times 2^n$ pixels. The authors [7] split image representation into 3 parts: quantum register for m colors (QSMC), quantum register for N coordinates (QSNC), and image storing. Authors provide the following intensity representation algorithm, which we reproduced in our repository.

If $|w_i\rangle$ is a pixel intensity representation and $|u_i\rangle$ is a pixel coordinate representation, then full pixel representation is $|\psi_i\rangle = |w_i\rangle \otimes |u_i\rangle$.

The paper proves the reliability of the method from the mathematical prospects. Moreover, the authors provide a quantum image compression algorithm and image segmentation based on extended Grover search [35]. The

method was not broadly utilized in quantum image processing and we could not find any publications based on it.

The main weakness of the method is the continuous approach to coordinate representation. When the number of pixels becomes bigger, even a small shift in probabilities affects the outcome. For example, IonQ QPU's R_y gate precision is $10^{-3}\pi$ radians [36], what makes impossible to encode coordinates of image larger than 512×512 . In this case the coordinate encoding error becomes significant and coordinate estimation precision decreases.

2.2.2 OQIM

The authors [13] provide a way to store classical images by intensity sorting. Firstly, authors map the ordered pixel intensities present in the image to numbers. Then the continuous representation defines pixel color and coordinate (θ and ϕ respectively). Figure 2d provides an example of the 2×2 .

The authors' idea is to utilize a single qubit for both intensity and coordinate. An additional qubit controls the mode of representation (coordinate or intensity). Thus, for the image represented in the figure 2a the following equation holds:

$$|I\rangle = \frac{1}{2^{3/2}} \left[\begin{aligned} &((\cos \theta_0 |0\rangle + \sin \theta_0 |1\rangle) |0\rangle + (\cos \phi_0 |0\rangle + \sin \phi_0 |1\rangle) |1\rangle) \otimes |00\rangle + \\ &((\cos \theta_1 |0\rangle + \sin \theta_1 |1\rangle) |0\rangle + (\cos \phi_1 |0\rangle + \sin \phi_1 |1\rangle) |1\rangle) \otimes |01\rangle + \\ &((\cos \theta_2 |0\rangle + \sin \theta_2 |1\rangle) |0\rangle + (\cos \phi_2 |0\rangle + \sin \phi_2 |1\rangle) |1\rangle) \otimes |10\rangle + \\ &((\cos \theta_3 |0\rangle + \sin \theta_3 |1\rangle) |0\rangle + (\cos \phi_3 |0\rangle + \sin \phi_3 |1\rangle) |1\rangle) \otimes |11\rangle \end{aligned} \right] \quad (6)$$

Authors propose the histogram specification process that allows to shift the image histogram. Authors provide "image comparison between two images and multiple images..., the parallel quantum searching" [37]. Paper also covers the multidimensional OQIM case. Basic algorithm implementation is available in our repository.

2.2.3 NAQSS

Authors' encoding approach [9] is similar to the QSMC and QSNQ (section 2.2.1). Encoding starts with color representation. If $color_i$ represents the i^{th} pixel color, then colors $\{color_1, color_2, \dots, color_M\}$ - a set of all possible colors for the image. Therefore rotation angle $\phi_i = \frac{\pi(i-1)}{2(M-1)}$ defines i^{th} state rotation angle. For the RGB image, each color value is $i = R \times 256 \times 256 + G \times 256 + B + 1$ what takes range from $color_1 = (0, 0, 0)$ to $color_{16777216} = (255, 255, 255)$.

The coordinate representation is the following. Suppose data has k dimensions (for flat image we assume $k = 2$). Then, each pixel sets in the following state:

$$|\psi_\phi\rangle = \sum_{i=0}^{2^n-1} a_i |v_1\rangle |v_2\rangle \dots |v_k\rangle \quad (7)$$

where $i = i_1 \dots i_j i_{j+1} \dots i_l \dots i_m \dots i_n$ is a binary expansion of the coordinate $v_1 = i_1 \dots i_j$, $v_2 = i_{j+1} \dots i_l$ and $v_k = i_m \dots i_n$ are the expansions of each coordinate separately.

The approach bases on a normalised intensity representation:

$$\theta = \frac{a_i}{\sqrt{\sum_{y=0}^{2^n-1} a_y^2}}, \quad (8)$$

where a_i is an intensity of current pixel i and $\sum_{i=0}^{2^n-1} \theta_i^2 = 1$.

Authors suggests to use image cropping and extend circuit by 1 qubit. The equation explains the cropped quantum image:

$$|\Psi\rangle = \sum_{i=0}^{2^n-1} \theta_i |v_1\rangle |v_2\rangle \dots |v_k\rangle |\chi_i\rangle \quad (9)$$

where $|\chi_i\rangle = \cos\gamma_i |0\rangle + \sin\gamma_i |1\rangle$, γ_i "represents the serial number of the sub-image which contains the pixel corresponding to the coordinate $|v_1\rangle |v_2\rangle \dots |v_k\rangle$ ". Simply – index of a sub-image.

The idea of image cropping index allows to retrieve a target sub-image (segmentation) from a quantum system. Additionally, a single qubit is a cheap way of color representation. Li *et al.* described image encryption based on normal arbitrary superposition state [38]. Based on geometric transformations of multidimensional color images based on normal arbitrary superposition state authors provide such transformations as two-point swapping, flip (uncluding local), orthogonal rotation, and translation [39]. Zhou and Sun proposed multidimensional color images similarity comparison for QNASS encoded images [40].

2.3 Pure discrete representation

Representation algorithms of this chapter utilizes only discrete amplitude encoding for both pixel intensity and coordinates. Methods described here utilizes the multicontrol CX -gate as in the figure 4.



Fig. 4: multi-control CX gate. Gate consists of 3 control qubits that apply NOT operation on the last one - target - qubit

2.3.1 NEQR

Authors [6] suggest to use full intensity binary expansion for image encoding. The most powerful thing of this explicitly encoded approach is the possibility to read intensity determinedly. The image with the intensity range 2^q (where q equals 8 in case of 256 intensity levels) is encoded in the following way:

$$|I\rangle = \frac{1}{2^n} \sum_{Y=0}^{2^n-1} \sum_{X=0}^{2^n-1} \bigotimes_{i=0}^{q-1} |C_{YX}^i\rangle |YX\rangle \quad (10)$$

Where $|C_{YX}^i\rangle$ and $|YX\rangle$ are intensity and coordinate expansions respectively. The same principle INCQI authors use in their paper [41].

Figure 2e represents an example of the image encoded with NEQR. The algorithm code is available in the repository.

Apart from determinism, the NEQR has several advantages. The paper says about "partial color operations and statistical color operations" [6]. The authors of the described paper split all possible image operations into 3 groups:

- Complete Intensity Operations (CC): changes pixel's intensity in a whole image or it's area.
- Partial Intensity Operations (PC): changes intensity of pixels in the certain gray-scaled range.
- Color Statistical Operation (CS): computes intensity statistics.

Authors extended approach to the log-polar images in QUALPI [42] (figure 2f shows the encoding example). Additionally, such comprehensive processing as complement intensity transformation and upscaling are also described in the book [19].

Next, strong point of the NEQR is a more efficient circuit compression algorithm. The Espresso Boolean expressions compression [43] is a base for this algorithm. While FRQI algorithm compression ratio is 50% of utilized gates, NEQR allows to reduce the number of gates by 75%.

The negative side appears from the determinant approach. Each intensity expansion leads to utilizing as much qubits as the length of the expansion. Thus, the quantum circuit depth increases proportionally to the image intensity resolution. However image size increases the number of utilized qubits only logarithmically.

As a result, NEQR is useful for reliable intensity representation, supports large images and comprehensive processing. The approach is less applicable for data with high intensity resolution. However this encoding approach is bountiful in terms of processing techniques. For instance, identification of desired pixels in an image using Grover's quantum search algorithm [44], edge extraction based on Laplacian operator [45], scaling [46], least squares filtering [47], morphological gradient [48], edge extraction based on classical Sobel operator [49], quantum image histogram [50], edge extraction based on improved Prewitt operator [51], mid-point filter [52] dual-threshold quantum image segmentation [53], steganography based on least significant bit [54], erosion

and dilation [55]. Finally, the same encoding method is used for LSB-Based quantum audio watermarking [56].

	00	01	10	11
0	0	128	255	
1				

Fig. 5: Non-square image, empty cells are expanding to powers of 2

2.3.2 GQIR

The authors [10] refer to the NEQR approach (section 2.3.1) and suggest an approach to represent nonsquare images. Figure 5 represents the possible nonsquare image with binary intensity expansions 00000000, 10000000, and 11111111 respectively for each pixel.

As far as 3 qubits are able to represent up to 4×2 images, therefore 5 states out of 8 are redundant. To keep measured image shape the same as input's, the authors do not encode pixels without intensity value and leave them to have black color with 0 qubit amplitude. This advantage allows to represent images of an arbitrary shape.

The authors suggest image up-scaling based on the nearest-neighbor method. In addition, Zhu *et al.* provided encryption scheme [57], Zhou and Wan implemented image scaling based on bilinear interpolation [58], Zhang *et al.* extended approach to floating-point quantum representation and proposed two rows interchanging and swap operations [59]. We implemented GQIR representation method in our repository.

2.3.3 QRMW

The authors [11] provide the representation approach for multichannel images. Each channel corresponds to a specific wavelength. QRMW allows "to encode the color values corresponding to the respective wavelength channel of the pixels in the image".

The equation below defines the intensity of each pixel located in the x, y, λ coordinates (where λ represents wavelength channel index):

$$\begin{aligned}
 f(\lambda, y, x) &= c_{\lambda_{yx}}^0, c_{\lambda_{yx}}^1, \dots, c_{\lambda_{yx}}^{q-2}, c_{\lambda_{yx}}^{q-1}, \\
 f(\lambda, y, x) &\in [0, 2^q - 1], \quad c_{\lambda_{yx}}^k \in [0, 1],
 \end{aligned} \tag{11}$$

where $2^q - 1$ is the maximum amplitude of any wavelength. Then, the QRMW image representation is the following:

$$|I\rangle = \frac{1}{\sqrt{2^{b+n+m}}} \sum_{\lambda=0}^{2^b-1} \sum_{y=0}^{2^n-1} \sum_{x=0}^{2^m-1} |f(\lambda, y, x)\rangle \otimes |\lambda\rangle \otimes |yx\rangle, \quad (12)$$

where b defines the number of channels. As a results, the method contains the extended realization of NEQR (2.3.1). In addition, the authors describe image compression, complete and partial color operations, and position operations. The same authors presented the edge detection algorithm [60] and extended their encoding approach to the multichannel audio representation [61].

2.3.4 BRQI

The authors [12] suggest to split image into n bitplanes where n is a resolution of the pixel intensity. Encoding proceeds through availability of the current bitplane in the pixel with current coordinates.

Suppose an example of the gray-scaled 2×2 image with the following pixel intensities: $\{0, 125, 200, 255\}$. The binary expansion for pixel-wise intensity is the following: 00000000, 01111101, 11001000, 11111111. Taking bits from each expansion, one can receive 8 bitplanes as in the figure 6.

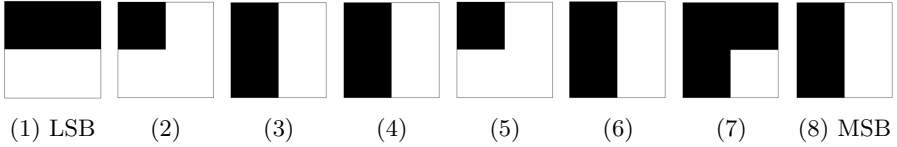


Fig. 6: Bitplane image representation, each letter corresponds to the number of biplane. The first and the last bit for each bitplane have special names "the least significant bit" (LSB) and "the most significant bit" (MSB) respectively.

This paper was inspired by general NEQR approach and defines j^{th} bitplane as follows:

$$|\Psi^j\rangle = \frac{1}{\sqrt{2^n}} \sum_{x=0}^{2^{n-k}-1} \sum_{y=0}^{2^k-1} |g(x, y)\rangle |x\rangle |y\rangle \quad (13)$$

where j - denotes the bitplane index ($j = 0, \dots, 7$), $g(x, y) \in \{0, 1\}$ shows presence or absence of a bit in j^{th} bitplane. As a result, the qubit scheme consists of X-, Y-coordinate qubits, bitplane qubits and 1 target qubit, showing availability of the bitplane's current bit. The encoding method is implemented in our repository.

BRQI supports processing operations: bitplane interchange, translation and intensity operation. Heidari *et al.* proposed selective encryption for the BRQI encoded information [62]. Recently, Khorrampanah *et al.* proposed RGB images encryption [63]. The work of Mastriani, 2015 [64] deserves special attention, as it describes Quantum Boolean (QuBo) image denoising based on image bitplane splitting. The same paper explains the Classical-to-quantum (C2QI) and Quantum-to-classical interfaces (Q2CI). Later Mastriani

proves [65] reliability of the bitplane splitting approach in term of C2QI and Q2CI.

To conclude, the BRQI is a promising method in terms of image representation and processing. At the same time, the technique is built upon the NEQR, thus the number of qubit remains in dependence on the intensity resolution.

2.3.5 QIIR

Indexed images consist of 2 tables: combination of the channel values (first table) and pointers to the palette matrix (second table). An example of such an image is in the figure 7. Authors [14] encode both image's tables ($|Q_{Data}\rangle$ and $|Q_{Map}\rangle$) using NEQR.

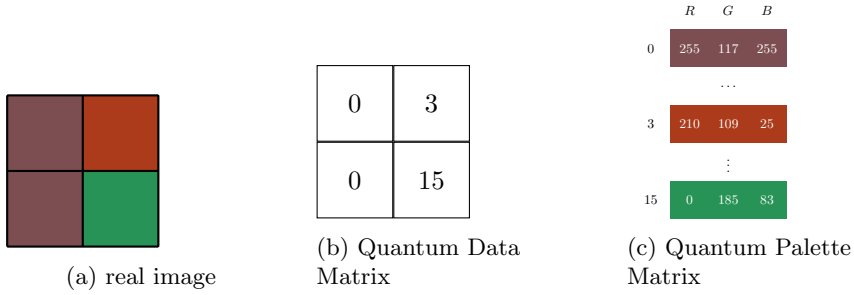


Fig. 7: QIIR image representation

2.3.5.1 Quantum Data Matrix

In order to encode $2^n \times 2^n$ Q_{Data} matrix, authors apply NEQR 2.3.1 approach. If (Y, X) is a cell location, I_{YX} is a cell value, then expression is the following:

$$|Q_{Data}\rangle = \frac{1}{2^n} \sum_{Y=0}^{2^n-1} \sum_{X=0}^{2^n-1} |I_{YX}\rangle \otimes |YX\rangle \quad (14)$$

2.3.5.2 Quantum Palette Matrix

The authors use the same NEQR 2.3.1 approach to encode the color palette. In case of RGB encoding 24 qubits are reserved: 8 for each color. Following equation describes the palette matrix encoding.

$$|Q_{Map}\rangle = \frac{1}{\sqrt{2^q}} \sum_{j=0}^{2^q-1} |C_j\rangle \otimes |j\rangle \quad (15)$$

Authors provide several processing techniques such as R_y rotation on 90° , cyclic shift, color inversion, color replacement, color look-up, steganography. Besides the authors' suggested processing techniques, no other images handling procedures exist from the best of our knowledge.

The number of utilized qubits is a major disadvantage of the method, as the data literally consist of 2 images.

2.4 Phase representation. FTQR

Grigoryan and Aganyan offer phase-based image encoding [15].

$$|\check{f}\rangle = \frac{1}{\sqrt{N}} \sum_{k=0}^{N-1} e^{i\alpha f_k} |k\rangle \quad (16)$$

where $\alpha = 2\pi/1024$. The term $e^{i\alpha f_k} |k\rangle$ allows to map classical intensity values $(0, 255)$ into imaginary plane $(x + i \cdot y)$. Here f_k is in input signal in the coordinate k which expands to x and y . In this way the representation is following:

$$|\check{f}\rangle = \frac{1}{\sqrt{MN}} \sum_{m=0}^{M-1} \sum_{n=0}^{N-1} e^{i\alpha f_{n,m}} |n, m\rangle \quad (17)$$

Authors do not provide any processing techniques but extend the approach up to multidimensional images. The image representation did not take share in the processing techniques research due to its novelty from our opinion. The method is purely phase based, and for measurement it needs phase-to-amplitude transformation. This fact implies additional computation resources.

3 Discussion and conclusion

We reviewed 14 method of image encoding and propose to categorize them according to classification in figure 1. Most of them have the common specific disadvantage, which comes from the quantum computing nature: it is impossible to measure all the pixels in a single trial. For continuous methods, the intensity estimation precision depends on the number of trials. Discrete methods allow to derive information only about 1 pixel from 1 shot. Figure 8 represents the comparison of three metrics for the selected algorithms implemented in our repository: circuit depth, qubit number, and quantum volume.

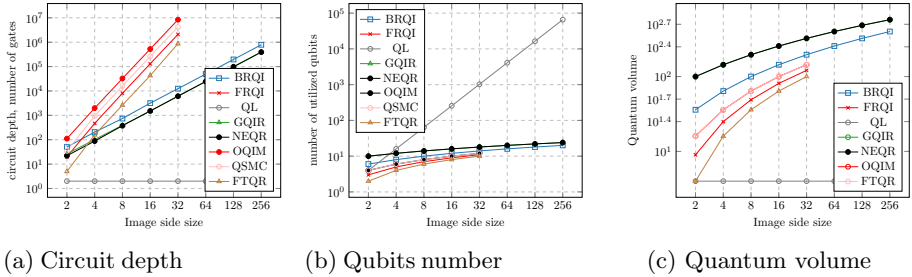


Fig. 8: Metrics

Tables A1, A2, A3 with columns representing image side size show the same metrics.

We observed that majority of techniques utilize a similar number of qubits, however the circuit depth shows the highest values for continuous and phase

representations and the lowest for the Qubit Lattice approach. The continuous and phase representations are so heavy in depth that we could not execute circuits for images bigger than 32×32 . Moreover, for all approaches, we could not succeed in real IBM-Washington [66] and IonQ [36] QPU simulation where depth reaches 10^5 for the images of size 4×4 and 8×8 for each machine respectively. This happened because of the multicontrolled rotation gate, which is a base for all continuous and phase methods, is itself expensive for implementation. Following that, it is computationally expensive to simulate high resolution images encoding, especially for continuous and approaches. Additionally, we did not succeed to measure FTQR, and as a result, we were unable to check whether representation works in the full encoding-decoding pipeline correctly. However, FTQR shows the minimum growth of utilized qubits and quantum volume numbers. Considering the number of qubits, Qubit Lattice is the most inappropriate representation algorithm even for IBM-Washington, as qubits can represent at most 8×8 images. Discrete representations stand in between, therefore, is the most promising group of image representation algorithms.

Each method has its own features. For example, some authors constructed their methods to encode a specific type of image (log-polar, multi-wavelength, indexed). Other authors made an accent on the representation way (based on bitplanes, Fourier transform, order-encoding). While some authors describe their approach in terms of quantum state normality (NAQSS), others operated on color and coordinate differentiation (QSMC and QSNQ). This fact might explain the huge number of processing types for the NEQR 2.3.1 and FRQI 2.1.2 representations. Both of them are general, intuitive and appear as main representative for the discrete and continuous groups respectively. Still, NEQR "could perform the complex and elaborate color operation more conveniently than FRQI" [67] due to obvious both – coordinate and pixel intensity encoding.

The image processing techniques significantly impact image representations. The majority of the discussed methods come with processing algorithms. And yet, the overall stack of available processing is not full. Such comprehensive tools as segmentation, feature extraction, machine learning, recognition keep poor and imperfect review. At the same time, research in these branches actively move these topics forward. Thus, opinion about quantum image processing as a "quantum hoax" [68] seems like a matter of time.

We assign our next work to the problems of the image processing in the perspective of machine learning applications. Convolutions, pooling, statistics calculation, and multi-image processing are in the scope of the future work. We are also inspired for further research of the image representation algorithms.

Declarations

Code availability

The python code is available in the GitHub repository <https://github.com/UralmashFox/QPI>.

Authors' contributions

Marina Lisnichenko - had the idea for the article, performed the literature search and data analysis. Stanislav Protasov - critically revised the work.

Data availability

Data sharing not applicable to this article as no datasets were generated or analysed during the current study.

Ethics approval and consent to participate

Not applicable

Human and Animal Ethics

Not applicable

Consent for publication

Not applicable

Competing interests

The authors have no conflicts of interest to declare that are relevant to the content of this article.

Funding

No funds, grants, or other support was received.

Acknowledgements

Not applicable

Authors' information



Marina Lisnichenko received the M.S. in robotics from Innopolis University in 2021. She is currently pursuing the PhD degree with the Machine Learning and Knowledge Representation lab, Innopolis University. Her research interests include quantum information processing, quantum circuit compression, geographic information processing.



Stanislav Protasov received the PhD degree in the computer science from Voronezh State University in 2013. He is currently an Associate Professor with Innopolis University. His research interests include applied machine learning, information retrieval, applications of quantum computing, quantum state preparation.

Appendix A Metrics tables

Table A1: Circuit depth

Image encoding	2	4	8	16	32	64	128	256
BRQI	50	206	738	3164	12400	49218	195902	784866
FRQI	467	8003	130307	2094083	—	—	—	—
QL	2	2	2	2	2	2	2	2
GQIR	26	102	389	1491	6180	24511	98014	392236
NEQR	22	88	375	1513	6075	24410	97923	392281
OQIM	111	1983	32511	523263	8382466	—	—	—
QSMC	35	943	16063	260863	4189183	—	—	—
FTQR	5	158	2635	42813	869016	—	—	—

Table A2: Number of utilized qubits

Image encoding	2	4	8	16	32	64	128	256
BRQI	6	8	10	12	14	16	18	20
FRQI	3	5	7	9	11	—	—	—
QL	4	16	64	256	1024	4096	16384	65536
GQIR	10	12	14	16	18	20	22	24
NEQR	10	12	14	16	18	20	22	24
OQIM	4	6	8	10	12	—	—	—
QSMC	4	6	8	10	12	—	—	—
FTQR	4	6	8	10	—	—	—	—

Table A3: Quantum volume

Image encoding	2	4	8	16	32	64	128	256
BRQI	36	64	100	144	196	256	324	400
FRQI	9	25	49	81	121	—	—	—
QL	4	4	4	4	4	4	4	4
GQIR	100	144	196	256	324	400	484	576
NEQR	100	144	196	256	324	400	484	576
OQIM	16	36	64	100	144	—	—	—
QSMC	16	36	64	100	144	—	—	—
FTQR	4	16	36	64	100	—	—	—

References

- [1] Leprince-Ringuet, D.: Daphne Leprince-Ringuet: Quantum Computing Is at an Early Stage. But Investors Are Already Getting Excited. <https://www.zdnet.com/article/quantum-computing-is-at-an-early-stage-but-investors-are-already-getting-excited/>
- [2] Venegas-Andraca, S.E., Bose, S.: Storing, processing, and retrieving an image using quantum mechanics. In: Quantum Information and Computation, vol. 5105, pp. 137–147 (2003). <https://doi.org/10.1117/12.485960>. International Society for Optics and Photonics
- [3] Latorre, J.I.: Image compression and entanglement. arXiv preprint quant-ph/0510031 (2005). <https://doi.org/10.48550/arXiv.quant-ph/0510031>
- [4] Le, P.Q., Dong, F., Hirota, K.: A flexible representation of quantum images for polynomial preparation, image compression, and processing operations. Quantum Information Processing **10**(1), 63–84 (2011). <https://doi.org/10.1007/s11128-010-0177-y>
- [5] Sun, B., Le, P.Q., Iliyasu, A.M., Yan, F., Garcia, J.A., Dong, F., Hirota, K.: A multi-channel representation for images on quantum computers using the $\text{rgb}\alpha$ color space. In: 2011 IEEE 7th International Symposium on Intelligent Signal Processing, pp. 1–6 (2011). <https://doi.org/10.1109/WISP.2011.6051718>. IEEE
- [6] Zhang, Y., Lu, K., Gao, Y., Wang, M.: Neqr: a novel enhanced quantum representation of digital images. Quantum information processing **12**(8), 2833–2860 (2013). <https://doi.org/10.1007/s11128-013-0567-z>
- [7] Li, H.-S., Qingxin, Z., Lan, S., Shen, C.-Y., Zhou, R., Mo, J.: Image storage, retrieval, compression and segmentation in a quantum system. Quantum information processing **12**(6), 2269–2290 (2013). <https://doi.org/10.1007/s11128-012-0521-5>
- [8] Yuan, S., Mao, X., Xue, Y., Chen, L., Xiong, Q., Compare, A.: Sqr: a simple quantum representation of infrared images. Quantum Information Processing **13**(6), 1353–1379 (2014). <https://doi.org/10.1007/s11128-014-0733-y>
- [9] Li, H.-S., Zhu, Q., Zhou, R.-G., Song, L., Yang, X.-j.: Multi-dimensional color image storage and retrieval for a normal arbitrary quantum superposition state. Quantum Information Processing **13**(4), 991–1011 (2014). <https://doi.org/10.1007/s11128-013-0705-7>

- [10] Jiang, N., Wang, J., Mu, Y.: Quantum image scaling up based on nearest-neighbor interpolation with integer scaling ratio. *Quantum information processing* **14**(11), 4001–4026 (2015). <https://doi.org/10.1007/s11128-015-1099-5>
- [11] Şahin, E., Yilmaz, I.: Qrmw: quantum representation of multi wavelength images. *Turkish Journal of Electrical Engineering & Computer Sciences* **26**(2), 768–779 (2018). <https://doi.org/10.3906/elk-1705-396>
- [12] Li, H.-S., Chen, X., Xia, H., Liang, Y., Zhou, Z.: A quantum image representation based on bitplanes. *IEEE Access* **6**, 62396–62404 (2018)
- [13] Xu, G., Xu, X., Wang, X., Wang, X.: Order-encoded quantum image model and parallel histogram specification. *Quantum Information Processing* **18**(11), 1–26 (2019). <https://doi.org/10.1007/s11128-019-2463-7>
- [14] Wang, B., Hao, M.-q., Li, P.-c., Liu, Z.-b.: Quantum representation of indexed images and its applications. *International Journal of Theoretical Physics* **59**(2), 374–402 (2020). <https://doi.org/10.1007/s10773-019-04331-0>
- [15] Grigoryan, A.M., Agaian, S.S.: New look on quantum representation of images: Fourier transform representation. *Quantum Information Processing* **19**(5), 1–26 (2020). <https://doi.org/10.1007/s11128-020-02643-3>
- [16] Oh, S., Choi, J., Kim, J.: A tutorial on quantum convolutional neural networks (qcn). In: 2020 International Conference on Information and Communication Technology Convergence (ICTC), pp. 236–239 (2020). IEEE
- [17] Cong, I., Choi, S., Lukin, M.D.: Quantum convolutional neural networks. *Nature Physics* **15**(12), 1273–1278 (2019). <https://doi.org/10.1038/s41567-019-0648-8>
- [18] Yang, C.-H.H., Qi, J., Chen, S.Y.-C., Chen, P.-Y., Siniscalchi, S.M., Ma, X., Lee, C.-H.: Decentralizing feature extraction with quantum convolutional neural network for automatic speech recognition. In: ICASSP 2021–2021 IEEE International Conference on Acoustics, Speech and Signal Processing (ICASSP), pp. 6523–6527 (2021). IEEE
- [19] Yan, F., Venegas-Andraca, S.E.: Quantum image processing (2020)
- [20] Caraiman, S., Manta, V.: Image processing using quantum computing. In: 2012 16th International Conference on System Theory, Control and Computing (ICSTCC), pp. 1–6 (2012). IEEE

- [21] Zhou, R.-G., Tan, C., Ian, H.: Global and local translation designs of quantum image based on frqi. *International Journal of Theoretical Physics* **56**(4), 1382–1398 (2017). <https://doi.org/10.1007/s10773-017-3279-9>
- [22] Thenmozhi, S., BalaSubramanya, K., Shrinivas, S., Joshi, S.K.D., Vikas, B.: Information hiding using quantum image processing state of art review. *Inventive Computation and Information Technologies*, 235–245 (2021). https://doi.org/10.1007/978-981-33-4305-4_18
- [23] Ma, H., He, Z., Xu, P., Dong, Y., Fan, X.: A quantum richardson–lucy image restoration algorithm based on controlled rotation operation and hamiltonian evolution. *Quantum Information Processing* **19**(8), 1–14 (2020). <https://doi.org/10.1007/s11128-020-02723-4>
- [24] Tariq Jamal, A., Abdel-Khalek, S., Ben Ishak, A.: Multilevel segmentation of medical images in the framework of quantum and classical techniques. *Multimedia Tools and Applications*, 1–14 (2021). <https://doi.org/10.1007/s11042-020-10235-7>
- [25] Farina, T.: Creating hybrid images using a quantum computer. PhD thesis, UNION COLLEGE (2021)
- [26] Sanchez, M., Sun, G.-H., Dong, S.-H.: Correlation property of multipartite quantum image. *International Journal of Theoretical Physics* **58**(11), 3773–3796 (2019). <https://doi.org/10.1007/s10773-019-04247-9>
- [27] Liu, X., Xiao, D.: Multimodality image fusion based on quantum wavelet transform and sum-modified-laplacian rule. *International Journal of Theoretical Physics* **58**(3), 734–744 (2019). <https://doi.org/10.1007/s10773-018-3971-4>
- [28] Hu, W.-W., Zhou, R.-G., Luo, J., Jiang, S.-X., Luo, G.-F.: Quantum image encryption algorithm based on arnold scrambling and wavelet transforms. *Quantum Information Processing* **19**(3), 1–29 (2020). <https://doi.org/10.1007/s11128-020-2579-9>
- [29] Yan, F., Jiao, S., Ilyyasu, A.M., Jiang, Z.: Chromatic framework for quantum movies and applications in creating montages. *Frontiers of Computer Science* **12**(4), 736–748 (2018). <https://doi.org/10.1007/s11704-018-7070-8>
- [30] Yan, F., Ilyyasu, A.M., Jiao, S., Yang, H.: Audio-visual synchronisation in quantum movies. In: 2018 IEEE 5th International Congress on Information Science and Technology (CiSt), pp. 274–278 (2018). IEEE
- [31] Sun, B., Ilyyasu, A.M., Yan, F., Sanchez, J.A.G., Dong, F., Al-Asmari, A.K., Hirota, K.: Multi-channel information operations on quantum

- images. *Journal of Advanced Computational Intelligence and Intelligent Informatics* **18**(2), 140–149 (2014)
- [32] Shende, V.V., Bullock, S.S., Markov, I.L.: Synthesis of quantum-logic circuits. *IEEE Transactions on Computer-Aided Design of Integrated Circuits and Systems* **25**(6), 1000–1010 (2006). <https://doi.org/10.1145/1120725.1120847>
- [33] Ma, G., Li, H., Zhao, J.: Quantum radon transform and its application. arXiv preprint arXiv:2107.05524 (2021)
- [34] Ding, M., Huang, T.-Z., Ji, T.-Y., Zhao, X.-L., Yang, J.-H.: Low-rank tensor completion using matrix factorization based on tensor train rank and total variation. *Journal of Scientific Computing* **81**(2), 941–964 (2019). <https://doi.org/10.1007/s10915-019-01044-8>
- [35] Grover, L.K.: Quantum computers can search arbitrarily large databases by a single query. *Physical review letters* **79**(23), 4709 (1997)
- [36] IonQ: Best Practices for Using IonQ Hardware: <https://ionq.com/best-practices>
- [37] Guanlei, X., Xiaogang, X., Xun, W., Xiaotong, W.: A novel quantum image parallel searching algorithm. *Optik* **209**, 164565 (2020). <https://doi.org/10.1016/j.ijleo.2020.164565>
- [38] Li, H.-S., Li, C., Chen, X., Xia, H.: Quantum image encryption based on phase-shift transform and quantum haar wavelet packet transform. *Modern Physics Letters A* **34**(26), 1950214 (2019). <https://doi.org/10.1142/S0217732319502146>
- [39] Fan, P., Zhou, R.-G., Jing, N., Li, H.-S.: Geometric transformations of multidimensional color images based on nass. *Information Sciences* **340**, 191–208 (2016)
- [40] Zhou, R.-G., Sun, Y.-J.: Quantum multidimensional color images similarity comparison. *Quantum Information Processing* **14**(5), 1605–1624 (2015). <https://doi.org/10.1007/s11128-014-0849-0>
- [41] Su, J., Guo, X., Liu, C., Lu, S., Li, L.: An improved novel quantum image representation and its experimental test on ibm quantum experience. *Scientific Reports* **11**(1), 1–13 (2021). <https://doi.org/10.1038/s41598-021-93471-7>
- [42] Zhang, Y., Lu, K., Gao, Y., Xu, K.: A novel quantum representation for log-polar images. *Quantum information processing* **12**(9), 3103–3126 (2013). <https://doi.org/10.1007/s11128-013-0587-8>

- [43] Brayton, R.K., Hachtel, G.D., McMullen, C., Sangiovanni-Vincentelli, A.: Logic Minimization Algorithms for VLSI Synthesis vol. 2. Springer, ??? (1984)
- [44] Iqbal, B., Singh, H.: Identification of desired pixels in an image using grover's quantum search algorithm. arXiv preprint arXiv:2107.03053 (2021). <https://doi.org/10.48550/arXiv.2107.03053>
- [45] Fan, P., Zhou, R.-G., Hu, W.W., Jing, N.: Quantum image edge extraction based on laplacian operator and zero-cross method. Quantum Information Processing **18**(1), 1–23 (2019). <https://doi.org/10.1007/s11128-018-2129-x>
- [46] Zhou, R.-G., Cheng, Y., Qi, X., Yu, H., Jiang, N.: Asymmetric scaling scheme over the two dimensions of a quantum image. Quantum Information Processing **19**(9), 1–20 (2020). <https://doi.org/10.1007/s11128-020-02837-9>
- [47] Wang, S., Xu, P., Song, R., Li, P., Ma, H.: Development of high performance quantum image algorithm on constrained least squares filtering computation. Entropy **22**(11), 1207 (2020). <https://doi.org/10.3390/e22111207>
- [48] Yang, J., Zhu, Y., Li, K., Yang, J., Hou, C.: Tensor completion from structurally-missing entries by low-tt-rankness and fiber-wise sparsity. IEEE Journal of Selected Topics in Signal Processing **12**(6), 1420–1434 (2018). <https://doi.org/10.1109/JSTSP.2018.2873990>
- [49] Fan, P., Zhou, R.-G., Hu, W., Jing, N.: Quantum image edge extraction based on classical sobel operator for neqr. Quantum Information Processing **18**(1), 1–23 (2019). <https://doi.org/10.1007/s11128-018-2131-3>
- [50] Heidari, S., Abutalib, M., Alkhambashi, M., Farouk, A., Naseri, M.: A new general model for quantum image histogram (qih). Quantum Information Processing **18**(6), 1–20 (2019). <https://doi.org/10.1007/s11128-019-2295-5>
- [51] Zhou, R.-G., Yu, H., Cheng, Y., Li, F.-X.: Quantum image edge extraction based on improved prewitt operator. Quantum Information Processing **18**(9), 1–24 (2019). <https://doi.org/10.1007/s11128-019-2376-5>
- [52] Ali, A.E., Abdel-Galil, H., Mohamed, S.: Quantum image mid-point filter. Quantum Information Processing **19**(8), 1–23 (2020). <https://doi.org/10.1007/s11128-020-02738-x>
- [53] Yuan, S., Wen, C., Hang, B., Gong, Y.: The dual-threshold quantum image segmentation algorithm and its simulation. Quantum

- Information Processing **19**(12), 1–21 (2020). <https://doi.org/10.1007/s11128-020-02932-x>
- [54] Zhou, R.-G., Luo, J., Liu, X., Zhu, C., Wei, L., Zhang, X.: A novel quantum image steganography scheme based on lsb. *International Journal of Theoretical Physics* **57**(6), 1848–1863 (2018). <https://doi.org/10.1007/s10773-018-3710-x>
- [55] Li, P., Shi, T., Lu, A., Wang, B.: Quantum circuit design for several morphological image processing methods. *Quantum Information Processing* **18**(12), 1–35 (2019). <https://doi.org/10.1007/s11128-019-2479-z>
- [56] Nejad, M.Y., Mosleh, M., Heikalabad, S.R.: An lsb-based quantum audio watermarking using msb as arbiter. *International Journal of Theoretical Physics* **58**(11), 3828–3851 (2019). <https://doi.org/10.1007/s10773-019-04251-z>
- [57] Zhu, H.-H., Chen, X.-B., Yang, Y.-X.: A multimode quantum image representation and its encryption scheme. *Quantum Information Processing* **20**(9), 1–21 (2021). <https://doi.org/10.1007/s11128-021-03255-1>
- [58] Zhou, R.-G., Wan, C.: Quantum image scaling based on bilinear interpolation with decimals scaling ratio. *International Journal of Theoretical Physics* **60**(6), 2115–2144 (2021). <https://doi.org/10.1007/s10773-021-04829-6>
- [59] Zhang, R., Xu, M., Lu, D.: A generalized floating-point quantum representation of 2-d data and their applications. *Quantum Information Processing* **19**(11), 1–20 (2020). <https://doi.org/10.1007/s11128-020-02895-z>
- [60] Şahin, E., Yilmaz, İ.: A quantum edge detection algorithm for quantum multi-wavelength images. *International Journal of Quantum Information* **19**(03), 2150017 (2021). <https://doi.org/10.1142/S0219749921500179>
- [61] Şahin, E., Yilmaz, İ.: Qrma: quantum representation of multichannel audio. *Quantum Information Processing* **18**(7), 1–30 (2019). <https://doi.org/10.1007/s11128-019-2317-3>
- [62] Heidari, S., Naseri, M., Nagata, K.: Quantum selective encryption for medical images. *International Journal of Theoretical Physics* **58**(11), 3908–3926 (2019). <https://doi.org/10.1007/s10773-019-04258-6>
- [63] Khorrampanah, M., Houshmand, M., Lotfi Heravi, M.M.: New method to encrypt rgb images using quantum computing. *Optical and Quantum Electronics* **54**(4), 1–16 (2022). <https://doi.org/10.1007/s11082-022-03581-3>

- [64] Mastriani, M.: Quantum boolean image denoising. *Quantum Information Processing* **14**(5), 1647–1673 (2015). <https://doi.org/10.1007/s11128-014-0881-0>
- [65] Mastriani, M.: Quantum image processing? *Quantum Information Processing* **16**(1), 1–42 (2017). <https://doi.org/10.1007/s11128-014-0881-0>
- [66] IBM: IBM-Washington Machine Details. https://quantum-computing.ibm.com/services?services=systems&order=qubits%20DESC&view=table&system=ibm_washington
- [67] Anand, A., Lyu, M., Baweja, P.S., Patil, V.: Quantum image processing. arXiv preprint arXiv:2203.01831 (2022). <https://doi.org/10.48550/arXiv.2203.01831>
- [68] Ruan, Y., Xue, X., Shen, Y.: Quantum image processing: opportunities and challenges. *Mathematical Problems in Engineering* **2021** (2021). <https://doi.org/10.1155/2021/6671613>